On tracer correlations in the troposphere: The case of ethane and propane

Yuhang Wang and Tao Zeng
School of Earth and Atmospheric Sciences, Georgia Institute of Technology, Atlanta, Georgia, USA

Received 14 May 2004; revised 6 October 2004; accepted 18 October 2004; published 22 December 2004.

[1] To investigate the reasons for and the utilities of tropospheric tracer correlations, we examine the interrelationship between ethane and propane on the basis of the observations at northern middle and high latitudes (TOPSE) and over the tropical Pacific (PEM-Tropics B) and the corresponding global three-dimensional chemical transport model (GEOS-CHEM) simulations. We chose to examine the correlation between propane and ethane/propane ratio because it is more sensitive to mixing and is less dependent on temperature than that between ethane and propane. We show that the correlation generally follows the one determined by chemical (loss) kinetics and that the deviation from the kinetics slope reflects the difference between ethane and propane in the effect of mixing relative to chemical loss. At northern middle and high latitudes the model is generally in agreement with the observations in February and March but simulates a wrong seasonal change of the correlation from March to May. The model appears to overestimate the transport from lower to middle latitudes and the horizontal transport and mixing at high latitudes in May. Over the tropical Pacific the model reproduces well the observed two-branch structure of the correlation. The discrepancy between observed and simulated correlation slope values appears to reflect an underestimate of continental convective transport at northern middle latitudes and an overestimate of latitudinal transport into the tropics. In addition, we show that the correlation can be used to define the subset of observations, in which the coupling between chemistry and transport is simulated reasonably well in the model. Using the subset of observed and simulated data for inverse modeling would reduce (systematic) biases introduced by systematic model transport errors. On the basis of this subset (March at middle latitudes and February–April at high latitudes), we find that the model underestimates the emissions of ethane and propane by 14 ± 5%. *INDEX TERMS:* 0368 Atmospheric Composition and Structure: Troposphere—constituent transport and chemistry; 0365 Atmospheric Composition and Structure: Troposphere—composition and chemistry; 0317 Atmospheric Composition and Structure: Chemical kinetic and photochemical properties; *KEYWORDS:* tracer correlation, photochemical clock, chemistry and transport

Citation: Wang, Y., and T. Zeng (2004), On tracer correlations in the troposphere: The case of ethane and propane, *J. Geophys. Res.*, *109*, D24306, doi:10.1029/2004JD005023.

1. Introduction

[2] Light nonmethane hydrocarbons (NMHCs) from anthropogenic sources in the atmosphere are removed mostly by OH oxidation. The time evolution of light NMHC concentrations or their ratios can be used to define a "photochemical clock" for the oxidation and transport processes [e.g., *Parrish et al.*, 1992, and references therein]. Various analyses have been applied to examine the observed correlations of NMHCs to infer oxidation or transport characteristics. We briefly describe three general approaches.

[3] The first approach explores the differential seasonal variations in the long-term observations of light NMHCs. For example, *Penkett et al.* [1993] suggested that OH is the dominant oxidant for the removal of straight-chain paraffins over the North Atlantic while other oxidants such as NO_3 are also important for branched-chain paraffins. *Goldstein et al.* [1995] applied estimated emission inventories and a global 3-D chemical transport model to analyze the seasonal variations of NMHC measurements at Harvard Forest to deduce the winter-summer OH ratio and the annual mean OH concentration at the site. Fundamentally this approach is in line with budget studies of box or 3-D model simulations and is therefore used most frequently among the three approaches.

[4] The second approach is to examine the correlations between NMHCs or their ratios. The method does not require long-term observations as does the first method. *Parrish et al.* [1992] used NMHC ratios because they realized that background mixing may distort the correlations between NMHCs, while the NMHC ratios are not affected if the background concentrations are negligible. *McKeen and Liu* [1993] and *McKeen et al.* [1996] further showed, using 3-D model simulations and aircraft observations, that the

0148-0227/04/2004JD005023$09.00

observed correlation between two NMHCs or their ratios is within the area bounded by the pure mixing and pure OH-oxidation lines. In their analyses, constant background NMHC concentrations were specified on the basis of the observations. Stratospheric tracer correlations, in contrast to those of the troposphere, can be explained without invoking local mixing with background concentrations [e.g., *Plumb and Ko*, 1992; *Avallone and Prather*, 1997].

[5] The third approach traces back to the work by *Junge* [1974], who suggested that RSD = $\frac{0.14}{\tau}$, where RSD is the relative standard deviation (standard deviation/mean concentration) and τ is the lifetime of the tracer. The Junge relationship assumes that transport is unimportant [*Ehhalt et al.*, 1998; *Jobson et al.*, 1998]. *Ehhalt et al.* [1998] extended the Junge relationship to RSD = $A\tau^{-b}$ to take into account of the effect of transport. They analyzed alkane observations from the Pacific Exploratory Mission (PEM) West B and 3-D model simulations to show that the exponent b is approximately 0.5. An alternative formulation by *Jobson et al.* [1998, 1999] is that $S_{lnX} = A'\tau^{-b'}$, where S_{lnX} is the standard deviation of the tracer concentration in log space. The physical interpretations of the exponents are the same for the two formulations. However, *Jobson et al.* [1999] suggested that their formulation works better for short-lived NMHCs, whose RSD can be larger than 1.

[6] The physical interpretation of the first approach is the most straightforward but it usually requires long-term measurements not available from aircraft observations. A well-understood meteorological environment is also required for the budget analysis. In comparison, the latter two approaches only assume that the chemical sources are collocated, although the aforementioned analyses of NMHCs were for either surface sites or lower tropospheric aircraft observations.

[7] We are interested in this work to examine how light NMHC observations from regional aircraft missions can be used to evaluate the emissions and the coupling of chemistry and transport in 3-D chemical transport model simulations. One data set is that of the Tropospheric Ozone Production about the Spring Equinox (TOPSE) experiment [*Atlas et al.*, 2003]. The photochemical environment changes rapidly from February to May and from middle to high latitudes [*Blake et al.*, 2003; *Cantrell et al.*, 2003; *Wang et al.*, 2003a] and hence it provides a challenging problem for correlation based studies.

[8] When applying the approach by *Jobson et al.* [1998] to the observed C_2–C_5 alkane concentrations (20 ppbv < O_3 < 100 ppbv), we find complex changes of the fitting coefficients as functions of month, latitude, and altitude. The lifetimes of alkanes by OH oxidations are estimated using monthly mean OH concentrations calculated by *Wang et al.* [2003a]. The results may be expected on the basis of model calculations by *Ehhalt et al.* [1998], who showed large variations of the fitting coefficients by latitude and altitude. We will not try to examine the reasons for the variations of those fitting coefficients in this work.

[9] In comparison, we find that the correlation between ethane and propane is much more robust. In order to magnify the mixing effect and reduce the variability due to the temperature dependence of OH oxidation (section 2), we examine instead the correlation between propane and ethane/propane ratio. Tropospheric tracer correlation is affected by both mixing and chemical processes [e.g., *McKeen and Liu*, 1993]. As noted by *Parrish et al.* [1992] and *McKeen et al.* [1996], the two processes have different effects on tracer concentrations compared to their ratios. Mixing with background (clean) air decreases the concentrations but does not alter the ratio of the two tracers when their background concentrations are negligible. If the two tracers have different lifetimes, chemical loss leads to decreases of both their concentrations and the ratio of short-lived to long-lived tracers.

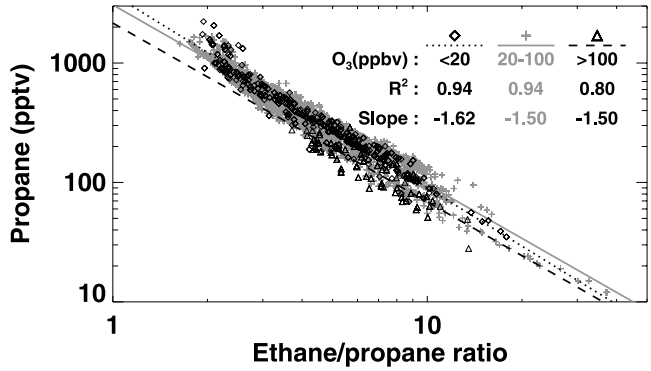

Figure 1. The correlations between propane and ethane/propane ratio during TOPSE. Three data groups for O_3 mixing ratios of <20, 20–100, and >100 ppbv are shown.

[10] We chose ethane and propane as chemical tracers in part because their sources are reasonably defined [e.g., *Wang et al.*, 1998b; *Xiao et al.*, 2004] and in part because higher alkane concentrations in the tropics are often below the detection limits. Figure 1 shows the correlations between propane and ethane/propane ratio for three types of air masses. When O_3 concentrations are less than 20 ppbv, the air mass is strongly influenced by halogen chemistry [*Evans et al.*, 2003; *Ridley et al.*, 2003; *Zeng et al.*, 2003]. When O_3 concentrations are higher than 100 ppbv, they are influenced by stratospheric air [*Browell et al.*, 2003; *Wang et al.*, 2003b]. Remarkably, the figure shows very tight correlations except some data points from the stratospherically influenced air masses and the slopes are very similar among the three different air masses.

[11] In section 2, we describe the difficulty in explaining the result of Figure 1 using currently established conceptual frameworks. We propose an alternative framework, which provides the conceptual basis for analyzing the observations and 3-D model results. Measurements and the GEOS-CHEM model are described briefly in section 3. Analyses of TOPSE and PEM-Tropics B observations and simulations are discussed in sections 4 and 5, respectively. Section 6 presents discussion and conclusions.

2. Conceptual Models

2.1. No Mixing

[12] We first examine the correlation between propane and ethane/propane ratio without considering the effect of mixing. The change of mixing ratio is driven by chemical loss

$$\frac{dX_i}{dt} = -l_i^c X \quad (i = 1, 2), \tag{1}$$

where X_1 and X_2 are the mixing ratios of ethane and propane, respectively, and l_i^c is the corresponding first-order chemical loss rate constant. The time evolution of the mixing ratio is then

$$X_i = X_i^0 \exp(-l_i^c t) \ (i = 1, 2), \tag{2}$$

where X_i^0 is the initial mixing ratio. The time evolution of ethane/propane ratio is

$$\frac{X_1}{X_2} = \frac{X_1^0}{X_2^0} \exp\left(-\left(l_1^c - l_2^c\right)t\right). \tag{3}$$

[13] The slope of propane (X_2) versus ethane/propane ratio (X_1/X_2) in log space, β, is therefore $-l_2^c/(l_2^c - l_1^c)$. Considering only oxidation by OH, the absolute linear slope, $|\beta|^c$,of the correlation of propane and ethane/propane ratio in log space is

$$|\beta|^c = \frac{k_2}{k_2 - k_1}, \tag{4}$$

where k_1 and k_2 are the reaction rate constants for OH oxidation of ethane and propane, respectively. We refer to this slope as the kinetics slope since it is solely determined by oxidation kinetics. When mixing is considered in the following sections, the absolute slope value deviates from $|\beta|^c$. We define $|\beta|$ as the absolute value of the general slope for the correlation of propane and ethane/propane ratio in log space (the mixing ratios of ethane and propane are always in pptv in this work). When only chemical oxidation is considered, $|\beta|$ and $|\beta|^c$ are interchangeable. On the basis of *Sander et al.* [2003], we find that $|\beta|^c = 1.24 \pm 0.07$ for a temperature range of -40 to 40°C when only OH oxidation is considered. The value of $|\beta|^c$ increases with temperature because the activation energy for OH oxidation of propane is lower than that for ethane.

[14] The kinetics slope of ethane-propane correlation, β', can be estimated similarly as k_2/k_1. The value of β' decreases from 6.7 to 4.3 as temperature increases from -40 to 40°C. The sensitivity of β' to temperature is much higher than that of $|\beta|$. We chose to examine the correlation between propane and ethane/propane ratio instead of that between ethane and propane because the former is more invariant with respect to temperature. Figure 1 shows that the average value of $|\beta|$ is 1.5 during TOPSE, higher than the $|\beta|^c$ value of 1.24 ± 0.07, reflecting the effect of mixing by dynamic processes.

2.2. Empirical Mixing Formulation

[15] Both mixing and chemical loss strongly affect the evolution of hydrocarbon concentrations [*McKeen et al.*, 1990; *Parrish et al.*, 1992; *McKeen and Liu*, 1993]. *McKeen et al.* [1996] approximated the concentration change as follows

$$\frac{dX}{dt} = -l^c X - l^m \left(X - X^b\right), \tag{5}$$

where l^m is the first-order mixing rate constant, and X^b is the background mixing ratio. The second term on the right-hand side represents the effect of mixing. *McKeen et al.* [1996] showed that the linear correlation between the mixing ratios of two alkanes holds true only in the region where their mixing ratios are much larger than their respective X^b values. Similarly analytical analysis of equation (5) shows that the deviation from linearity in the correlation between propane and ethane/propane ratio would occur when ethane or propane mixing ratios approach the same order of the corresponding background values.

[16] In comparison, we do not find any systematic deviations from the linear relationship in the observations toward the tail of the correlation in Figure 1 or in the same type of figures to be presented in the later sections. *McKeen et al.* [1996] noted the empirical nature of choosing the value of X^b. Furthermore, there is no a priori reason to assume that X^b values are constant. One way to reconcile the difference between equation (5) and the observations is to assume that X^b is a linear function of X

$$\frac{dX_i}{dt} = -l_i^c X_i - l_i^m (X_i - \alpha_i X_i), \tag{6}$$

where α_i is the linear coefficient for species i. Equation (2) is rewritten as

$$X_i = X_i^0 \exp\left[-\left(l_i^c + (1 - \alpha_i) l_i^m\right)t\right]. \tag{7}$$

If we further assume $l_1^m = l_2^m = l^m$ for ethane (i = 1) and propane (i = 2), we find that equation (4) becomes

$$|\beta| = \frac{k_2[\mathrm{OH}] + (1 - \alpha_2) l^m}{(k_2 - k_1)[\mathrm{OH}] + (\alpha_1 - \alpha_2) l^m}. \tag{8}$$

Now if we assume that $\alpha_1 = \alpha_2 = \alpha$ and consider that $k_2 \gg k_1$, we find that the mixing timescale $\tau_m = 1/l_m$ and the chemical lifetime of propane $\tau_{propane} = (k_2[\mathrm{OH}])^{-1}$ are in proportion:

$$\tau_m \approx \frac{1 - \alpha}{|\beta| - |\beta|^c} \ \tau_{propane}. \tag{9}$$

The upper limit of the mixing timescale is $\tau_m^{\max} = \tau_{propane}/(|\beta| - |\beta|^c)$. However, the appropriate value of α is not well defined. The physical interpretation of α is also difficult, preventing valuable inferences of physical insights from this calculation.

2.3. Turbulent Diffusion Based Empirical Formulation

[17] Using a turbulent diffusion based formulation may shed better light on the physical interpretation of the linear correlation shown in Figure 1. As in the model by *McKeen et al.* [1996], we consider a single plume. We also limit our discussion in one dimension. The chemical-diffusion equation in y direction of a Lagrangian frame moving with the mean wind can be written as

$$\frac{\partial X}{\partial t} = -l^c X - K \frac{\partial^2 X}{\partial y^2}, \tag{10}$$

where K is the eddy diffusion coefficient [e.g., *Seinfeld and Pandis*, 1998]. Considering dispersion to infinity, the analytical solution of an instant puff to equation (10) is

$$X(y, t) = \frac{Q}{2\sqrt{\pi K t}} \exp\left(-l^c t - \frac{y^2}{4Kt}\right), \tag{11}$$

where Q is the source of the instant puff. The solution does not in itself help our interpretation of Figure 1. Nor do the steady state solutions to equation (10) discussed by *McKenna* [1997] and *Ehhalt et al.* [1998].

[18] We propose here a finite-mixing model. The assumption is that the dispersion range in the atmosphere is not infinite as assumed in deriving equation (11), but finite. The dynamical nature of the finite-mixing model is complex and needs to be explored in a 3-D model setting. We will try to provide some physical interpretations later in the section. We emphasize that the rationale to develop a new conceptual model is not to predict the observations, but to facilitate our understanding of the observations and 3-D model results since currently established conceptual models do not explain the observations well.

[19] To separate the variables in equation (10), we define $X(t, y) = a(t)b(y)$. Hence we get

$$\frac{a'}{-l_c a} = \frac{b + K/l^c b''}{b} = \lambda. \tag{12}$$

The general solutions are

$$a(t) = A\exp(-\lambda l^c t), \tag{13}$$

$$b(y)'' = -\frac{l^c}{K}(\lambda - 1)b. \tag{14}$$

[20] For a finite dispersion range, the mixing ratio cannot decay away from the origin exponentially as long as the chemical lifetime of the species is not much shorter than the mixing timescale. The steady state solution ($\lambda = 1$) is unphysical for analyzing TOPSE and PEM-Tropics B observations (next section). Therefore the solution to equation (14) is physical only when $\lambda > 1$. We obtain

$$b(y) = B\sin\left(\sqrt{\frac{l^c}{k}(\lambda - 1)}\cdot y\right) + C\cos\left(\sqrt{\frac{l^c}{k}(\lambda - 1)}\cdot y\right).$$

Applying the above solution to ethane and propane and ignoring the oscillating variation of b(y), we obtain the absolute slope for the correlation of propane and ethane/propane ratio

$$|\beta| = \frac{\lambda_2 l_2^c}{\lambda_2 l_2^c - \lambda_1 l_1^c}. \tag{15}$$

As in equation (4), we consider only OH oxidation of ethane and propane

$$|\beta| = \frac{k_2}{k_2 - k_1 + (1 - \lambda_1/\lambda_2)k_1} \approx |\beta|^c\left(1 + \frac{(\lambda_1/\lambda_2 - 1)k_1}{k_2 - k_1}\right). \tag{16}$$

[21] The values of λ_1/λ_2 can be obtained on the basis of the observations (Figure 1) since all the other parameters are known. Relative to chemical loss, the effect of mixing for longer-lived ethane is larger than for propane and hence $\lambda_1 > \lambda_2$. As a result, we obtain $|\beta| > |\beta|^c$. This physical interpretation implies that as chemical lifetimes of ethane and propane decrease and OH concentrations increase from February to May in the TOPSE region, the value of $|\beta|$ would approach that of $|\beta|^c$. We would not expect any extreme deviation of $|\beta|$ from $|\beta|^c$ since the reaction of propane and OH is about 5 times faster than that of ethane and OH, i.e., $k_1/(k_2 - k_1) \approx 0.25$, in equation (16).

[22] One can alternatively use equation (13) as an empirical formula to replace that by *McKeen et al.* [1996] (equation (5)) to represent the effect of mixing on the correlation slope (equation (4)). We refer λ as the mixing augmentation factor. The finite-mixing model, however, could help the physical interpretation of the results. The difficulty due to mixing with background concentrations discussed previously in the formulation of equation (5) is no longer an issue. Mixing with background concentrations is now an initial-value problem rather than a boundary-value problem since mixing is only within finite regions. The decay time of background-mixing impact scales with the chemical lifetime. It would not lead to the deviation from the linear relationship as long as the initial plume concentration is much higher than the background value.

[23] Impermeable boundaries for mixing regions, such as that of the vortex in the wintertime Antarctic stratosphere, are rather difficult to define in the troposphere. A more realistic interpretation of the finite mixing model is that the region with high turbulent mixing is bounded by low turbulent mixing regions. The slow boundary mixing has a small effect on the tracer concentrations inside the high turbulent mixing region such that the correlation does not deviate from the linear line. A consequence is that one would expect coherent tracer correlations in the turbulent troposphere without reaching the global ''equilibrium slope'' proposed by *Plumb and Ko* [1992] for tracer correlations in the stratosphere.

[24] A second consequence of the finite-mixing model is that the results hold true only in regions sufficiently away from the sources such that the mixing processes have time to explore the dynamic boundaries. It is a necessary condition for $\lambda > 1$ in equation (14). In regions away from major sources of the tracers, the requirement for collocated sources is also relaxed due to mixing processes downwind from the emissions. For this reason, the TOPSE observations are well suited for the study of the correlation between propane and ethane/propane ratio since most air masses were chemically aged [*Atlas et al.*, 2003]. As *McKeen et al.* [1996], we make use of a 3-D chemical transport model to analyze the observations.

3. Observations and the Global Model

[25] Besides TOPSE observations, we also investigated the correlations between propane and ethane/propane ratio for three other aircraft field missions, PEM-Tropics A [*Hoell et al.*, 1999], PEM-Tropics B [*Raper et al.*, 2001], and the Transport and Chemical Evolution over the Pacific (TRACE-P) experiment [*Jacob et al.*, 2003]. The whole air samples of ethane and propane are analyzed by the same group [e.g., *Blake et al.*, 2003]. The measurement accuracy is the larger of 1% and 1.5 pptv.

[26] The correlation between propane and ethane/propane ratio is substantially better during TOPSE and PEM-Tropics B than TRACE-P and PEM-Tropics A (not shown). The results are expected on the basis of the finite mixing model. The latter two experiments took place near source regions,

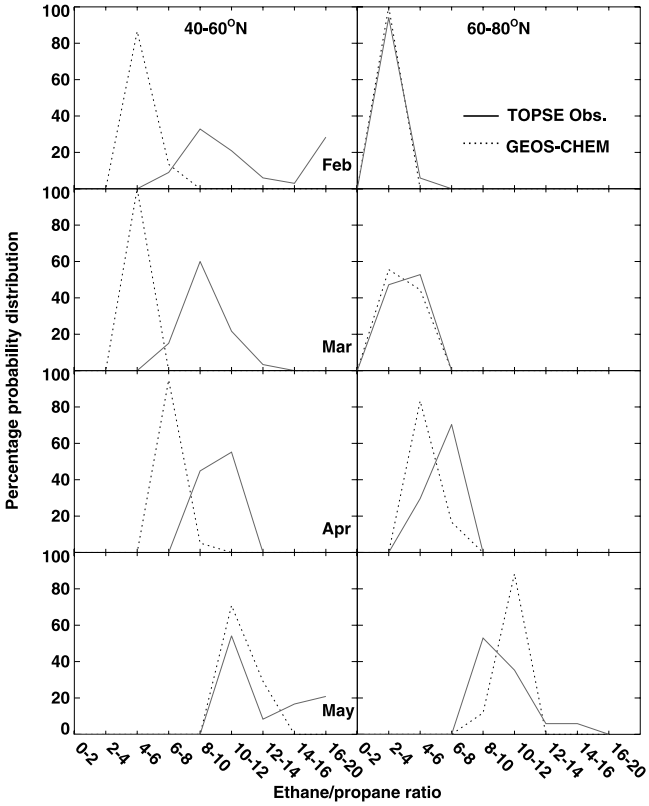

Figure 2. Observed and simulated probability distributions of ethane/propane ratio in the upper 10th percentile at middle and high latitudes from February to May during TOPSE. The selected observation data have O_3 mixing ratios between 20 and 100 ppbv to minimize the impact of halogen chemistry at low altitudes and transport from the stratosphere.

one off the east Asia coast [*Jacob et al.*, 2003] and the other downwind from relatively fresh biomass burning regions [*Schultz et al.*, 1999; *Talbot et al.*, 1999; *Wang et al.*, 2000]. In comparison, the former two experiments sampled more chemically aged air masses [*Raper et al.*, 2001; *Atlas et al.*, 2003]. In light of the results to be presented, there is potentially a wealth of information on emissions and transport that can be extracted by exploring the causes for the poor correlation between propane and ethane/propane ratio during TRACE-P and PEM-Tropics A. In this work, however, we will only focus on understanding the more robust correlations between propane and ethane/propane ratio observed during TOPSE and PEM-Tropics B experiments.

[27] The simulations of global tropospheric O_3-NO_x-hydrocarbon chemistry for year 2000 were conducted using the GEOS-CHEM model [*Bey et al.*, 2001] (version 5.05-03 is used). The (GEOS-3) meteorological fields for 2000 were assimilated by the NASA Global Model and Analysis Office (GMAO). More detailed description of the model and its applications can be found at http://www-as.harvard.edu/chemistry/trop/geos. Particularly worth of mentioning is the work by *Xiao et al.* [2004], who applied the correlations of methane with ethane and CO, respectively, to constrain the sources of methane on the basis of TRACE-P observations. In our simulations, the spatial resolution of the model is 4°x5° in the horizontal with 26 vertical layers in the troposphere. Industrial emissions are described by *Wang et al.* [1998a]. Biofuel combustion emissions are described by *Yevich and Logan* [2003]. Emissions from biomass burning are constrained by satellite observations for year 2000 [*Duncan et al.*, 2003]. We spun the model for a year with GMAO assimilated meteorological fields. The model was then run for January–May 2000 and the results were archived every hour.

4. Northern Middle and High Latitudes During TOPSE

[28] We investigate the seasonal and latitudinal evolution of propane and ethane/propane ratio correlation. From February to May, the photochemical environment changes rapidly as a function of month and latitude [*Wang et al.*, 2003a] and the concentrations of ethane and propane decrease significantly, particularly at higher latitudes [*Blake et al.*, 2003]. To filter out the effects of stratospheric transport and lower tropospheric halogen chemistry, only observations with O_3 concentrations between 20 and 100 ppbv are used.

[29] After inspecting the comparison results, we find that the model in general cannot reproduce the transport of relatively clean air masses to the TOPSE region. These air masses have high ethane/propane ratios because of the more rapid OH oxidation of propane than ethane. Figure 2 shows the monthly probability distributions of the upper 10th percentile of ethane/propane ratios at middle and high latitudes. From February to April, the simulated upper 10th percentile of ethane/propane ratios are significantly lower than the observations, suggesting that transport of clean air masses presumably from lower latitudes is too weak in the model. We find no evidence that the air masses with observed high ethane/propane ratios are due to Cl radical oxidation, which is not simulated in the model, on the basis of altitude distribution and the relative enhancements of alkanes to benzene of these data points compared to the rest of the data. The agreement is better in May. The long tails of high ethane/propane ratio data in some occasions significantly alter the calculated slope (β) between propane and ethane/propane ratio for the observations. We therefore only consider the data in the lower 90th percentile of ethane/propane ratios.

[30] Figure 3 shows the monthly correlations between propane and ethane/propane ratio for the selected observations and corresponding model simulations at middle and high latitudes. The correlation is tight in the observations and simulated results. However, the observed and simulated slopes can be quite different. Generally, the observed value of $|\beta|$ decreases from early spring toward summer as photochemistry becomes more active, qualitatively consistent with what we expect on the basis of equation (16). The seasonal trend is not as clear in GEOS-CHEM simulations because of the large $|\beta|$ values in May. The large deviations likely reflect problems in the transport characteristics since the photochemical activity change is driven mostly by increasing solar insolation [*Cantrell et al.*, 2003; *Wang et al.*, 2003a].

[31] Using the slope value, $|\beta|$, to evaluate the model results provides additional information that is not apparent by examining the simulated and observed medians. It should

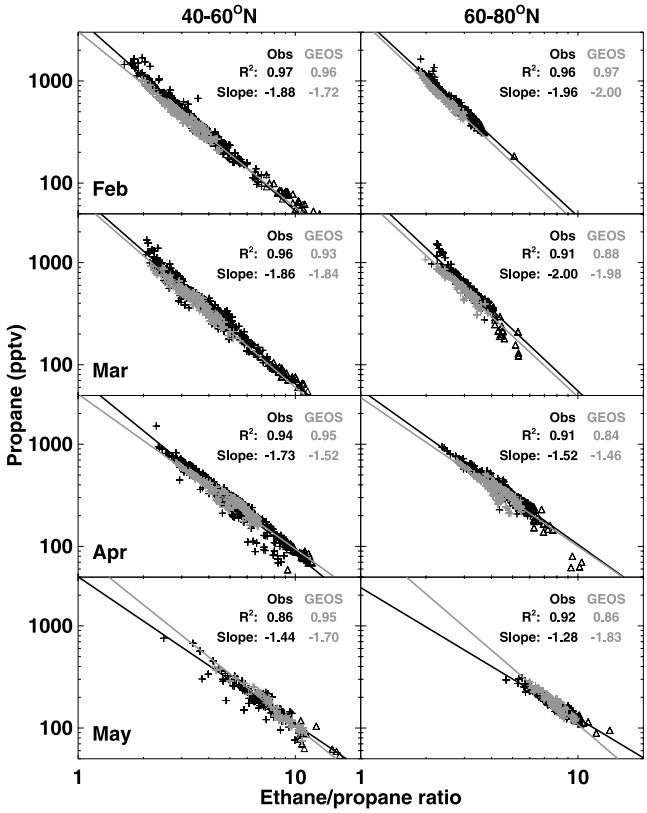

Figure 3. Observed and simulated correlations between propane and ethane/propane ratio for data with ethane/propane ratios in the lower 90th percentile as a function of latitude and month. Open triangles show observed data with ethane/propane ratios in the upper 10th percentile. The selected observation data have O_3 mixing ratios between 20 and 100 ppbv.

be noted that the evaluation is on a statistical basis, which is often required to evaluate the emissions of trace gases. To further illustrate this point, Figure 4 shows the monthly probability distributions of ethane/propane ratio at middle and high latitudes for the lower 90th percentile. The simulated probability distributions are in agreement with the observations at high latitudes and in February and March at middle latitudes. There is a seasonal shift of ethane/propane ratios toward higher values from March to May in the model and observations, reflecting increasing photochemical oxidation by OH. The shift is more apparent from April to May. The model overestimates the increase of the ethane/propane ratio at middle latitudes but is in agreement with the observations at high latitudes. In contrast, the corresponding decrease of $|\beta|$ values in the observations is not simulated in the model. On the basis of the finite-mixing model (section 2), the observations can be interpreted as the effect of mixing processes relative to photochemistry becomes less important in the observations from April to May, driving the $|\beta|$ value toward $|\beta|^c$ (equation (16)). However, mixing becomes more effective relative to photochemistry in the model from April to May, suggesting that the mixing processes in the model are overestimated.

[32] The overestimate of $|\beta|$ value (Figure 3) in May at middle latitudes is inconsistent with an overestimate of OH oxidation, but imply that transport from lower to middle latitudes is overestimated in the model. The overestimate of $|\beta|$ value coupled with a good agreement with the observed probability distribution of ethane/propane ratio in May at high latitudes likely implies excessive mixing within the region. The simulated vertical gradient of ethane is much higher than the observations in May at high latitudes (not shown), suggesting that vertical mixing is underestimated in the model. We hypothesize that the model horizontal transport and mixing are overestimated as a result because turbulent motions (in the vertical) driven by local convection would slow down mean westerly flows. Unfortunately the hypothesis cannot be tested in an off-line model like GEOS-CHEM.

[33] When 3-D chemical transport model simulations are used to constrain the emission sources on the basis of the observations, the model transport error if unknown is often assumed to be unbiased. As we show in Figure 3, the model transport error for TOPSE is clearly systematic particularly in May. Therefore comparing the observed and simulated $|\beta|$ values and the probability distributions of ethane/propane ratio provides an effective way to detect if the model results are systematically biased because of transport errors. In our case, Figure 3 suggests that the estimated emission inventory can be evaluated with better confidence using the TOPSE observations for March at middle latitudes and February–April at high latitudes. In these cases, the parallelization of observed and simulated correlation lines implies that the relative source difference can be calculated by the intercepts with any constant ethane/propane ratio

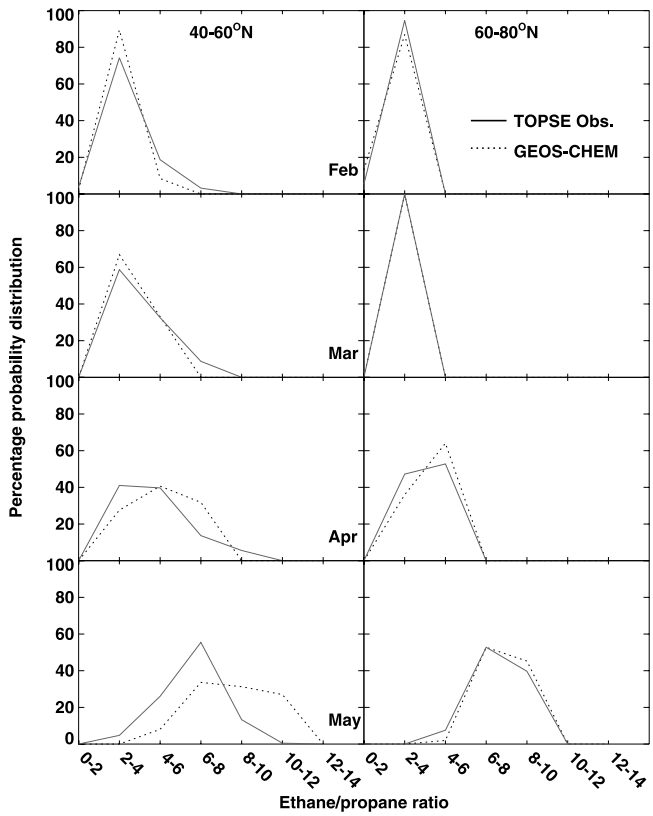

Figure 4. Same as Figure 2 but for ethane/propane ratios in the lower 90th percentile.

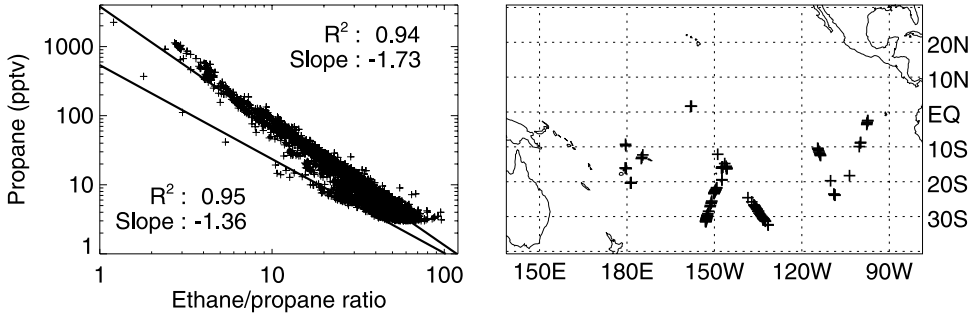

Figure 5. Observed correlations between propane and ethane/propane ratio during PEM-Tropics B. The right panel shows the locations of data points for the minor correlation branch (see text for details).

line. Employing only this subset is advantageous because one would otherwise need to know the ethane/propane emission ratio in order to calculate the difference between observed and simulated propane concentrations in freshly emitted plumes. We use the corresponding propane concentrations for the intercept of ethane/propane ratio of 1 to calculate an underestimate of 14 ± 5% in the model emissions of ethane and propane. For the other months at middle and high latitudes, depending on the range of ethane/propane ratios, the simulated propane concentrations can be higher or lower than the observations. For example, the best median value agreement between the model and observations are in May at middle latitudes, where there are large discrepancies in $|\beta|$ values (Figure 3) and the probability distributions of ethane/propane ratio (Figure 4). The estimates based on the correlation between propane and ethane/propane ratio are more robust because (1) it provides an objective criterion for selecting data groups that are better simulated by the model independent of the concentrations of ethane or propane; and (2) the results are consistent with both ethane and propane observations.

[34] The method has its limitations. First, the grouping of the data is empirical. In this analysis, we group the data by latitude and month because of the seasonal and latitudinal transition of solar insolation that drives photochemistry. We attempted to group the data by altitude. However, the results are not promising probably because there are no clearly defined stationary dynamical processes that would isolate ethane and propane concentrations to specific altitude ranges. The transient dynamical processes such as synoptic-scale weather systems, fronts, and convection often lead to vigorous vertical mixing. Second, applying the method requires that ethane and propane concentrations have reasonable large variations within each data group to define the slope value, $|\beta|$. As a result, data collected over sufficiently large spatial or temporal space must be grouped together. The results are meaningful only as statistics. The latter point is not necessarily a handicap for using the method to evaluate model performance because most model assessments are useful only as statistical means as well. Inverse modeling with 3-D chemical transport models [e.g., *Palmer et al.*, 2003; *Arellano et al.*, 2004] usually belongs to this category.

5. Tropical Pacific During PEM-Tropics B

5.1. Correlation Branching

[35] The PEM-Tropics B experiment took place over the tropical Pacific in March–April 1999 [*Raper et al.*, 2001]. Transport from the northern industrial regions to the tropical Pacific, particularly at lower altitudes, is the major sources of ethane, propane, and other hydrocarbons in the region [*Blake et al.*, 2001; *Wang et al.*, 2001]. Figure 5 shows the observed correlations between propane and ethane/propane ratio. There is a clear two-branch structure. The value of $|\beta|$ for the major correlation branch is 1.73, similar to the 1.7–1.9 values found at middle latitudes in March and April during TOPSE (Figure 3) and is generally consistent with the previous findings that the major fraction of hydrocarbons is transported from northern middle latitudes.

[36] The existence of a minor branch is very different from the TOPSE observations (Figure 3). To isolate the minor branch, we examine the deviations of data from the main correlation branch (Figure 6) and define the minor branch by data in the lower 5th percentile. By fitting only to these data, we find a minor slope with a smaller $|\beta|$ value of 1.4. The three data points with ethane/propane ratios <10 along the minor branch are found near the surface in the same location probably due to sampling of a fresh ship plume. Figure 5 also shows that the data points for the minor branch were sampled generally south of 10°S.

[37] It is not obvious what factors are responsible for the minor correlation. We make use of the GEOS-CHEM simulations described in section 3. The assimilated meteorology fields are for 2000 not 1999. The meteorological assimilation with GMAO GEOS-3 for 1999 is currently unavailable to us. A different meteorological year brings in

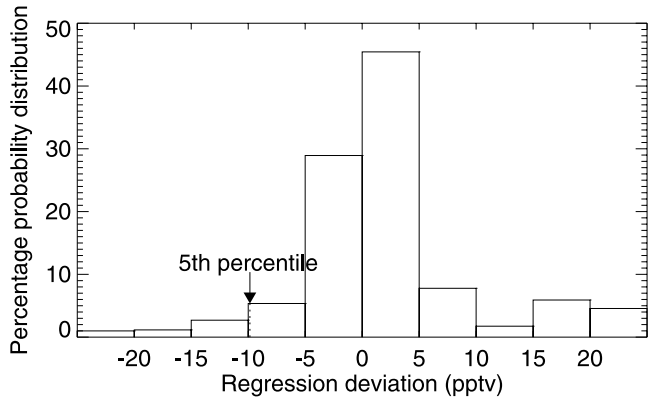

Figure 6. The probability distribution of propane mixing ratio deviations from the major correlation line in Figure 5.

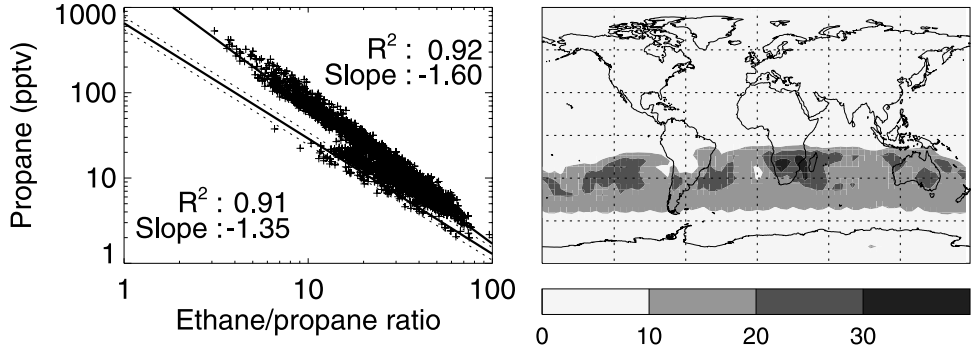

Figure 7. Simulated correlations between propane and ethane/propane ratio for PEM-Tropics B. The first of 50 synthetic data sets is shown. The right panel shows the percentages of data that fall into the region bounded by the dashed lines (±1 standard deviation around the minor correlation line) in the left panel.

our analysis additional uncertainties, which we will take into account in the discussion.

[38] The GEOS-CHEM model reproduces the two-branch structure (Figure 7). In the same manner as applied to the observational data, we can calculate the values of $|\beta|$ for the model results. To test the robustness of the results, we construct 50 synthetic data sets by randomly sampling the hourly model output in the same locations as the observations during the observation period. The resulting $|\beta|$ values are 1.60 ± 0.005 and 1.35 ± 0.04, for the major and minor correlations, respectively. Figure 7 also shows that the data for the minor branch in the model reside in the region at 10–40°S as found in the observations (Figure 5), suggesting that the minor correlation is due to emissions and associated atmospheric processing in the southern subtropical and middle latitudes. Compared to the observations, the model underestimates the $|\beta|$ value for the major branch but reproduces well the $|\beta|$ value for the minor branch suggesting better simulations of the processes contributing to the minor correlation.

[39] To further investigate the potential source contributions to the minor correlation, we conduct "tagged tracer" simulations, in which ethane and propane emitted by industry, biomass burning, and biofuel burning are simulated by separate chemical tracers. Hourly OH concentrations used in these simulations are archived from the full chemistry run. A total of 20 tracers are used. 16 are used to represent industrial ethane and propane emitted from 8 regions including North America, Europe, northern Asia (north of 30°N), southern Asia (south of 30°N), South America, northern Africa (north of the equator), southern Africa (south of the equator), and Australia. Inspection of the correlations between propane and ethane/propane ratio suggests that only 1 linear correlation line can be found for each source category. Therefore the secondary correlation in Figure 6 reflects a mixing regime for emissions over the southern subtropics and middle latitudes different from that for the more dominant northern industrial emissions.

[40] As previously, 50 synthetic data sets for each source category are constructed with randomly selected model data at the measurement locations. Table 1 shows the mean $|\beta|$ values for different source categories; the standard deviation is <0.005. It is clear that lower $|\beta|$ values are generally related to tagged tracers emitted in the southern subtropics, providing further evidence that the minor correlation is due to the interplay of transport and chemistry in that region.

5.2. Constraints of the Correlation on Convective Transport at Northern Middle Latitudes

[41] Convective transport generally plays an important role in the distribution of trace gas concentrations and we would expect that its effects are reflected in $|\beta|$ values. Furthermore, the parameterization of convective transport in the general circulation models is very uncertain [e.g., *Jacob et al.*, 1997]. Generally, short-lived chemical tracers, such as ^{222}Rn over land [e.g., *Jacob et al.*, 1997] and CH_3I over the ocean [e.g., *Bell et al.*, 2002], have been used to evaluate the convective characteristics of the models. However, the sources of these tracers are uncertain, and only limited observations are available. Direct comparison of model simulated and observed concentrations for these tracers often must be taken in the context of coarse spatial and temporal resolutions of the global models. It would be valuable if the observations of longer-lived species such

Table 1. Absolute Slopes of the Correlations Between Propane (pptv) and Ethane/Propane Ratio for Each Source Category in the Standard "Tagged Tracer" Simulation and That Without Convection[a]

Sources	$\|\beta\|$ Standard Simulation	$\|\beta\|$ No Convection
All sources[b]	1.60	1.44
Biomass	1.54	1.46
Biofuel	1.64	1.51
Industry (North America)	1.66	1.55
Industry (South America)	1.39	1.35
Industry (Europe)	1.68	1.52
Industry (North Africa)	1.49	1.44
Industry (South Africa)	1.35	1.33
Industry (North Asia)	1.65	1.47
Industry (South Asia)	1.51	1.44
Industry (Australia)	1.44	1.37

[a]The latitudinal border between northern and southern Africa is the equator; that between northern and southern Asia is 30°N. The model was run for one year first. The March and April results corresponding to the PEM-Tropics B period of the second year are used. Fifty synthetic data sets are generated by randomly sampling the hourly model output in the same locations as the observations. The mean absolute slopes are listed. The standard deviations are <0.005.

[b]For the major correlation.

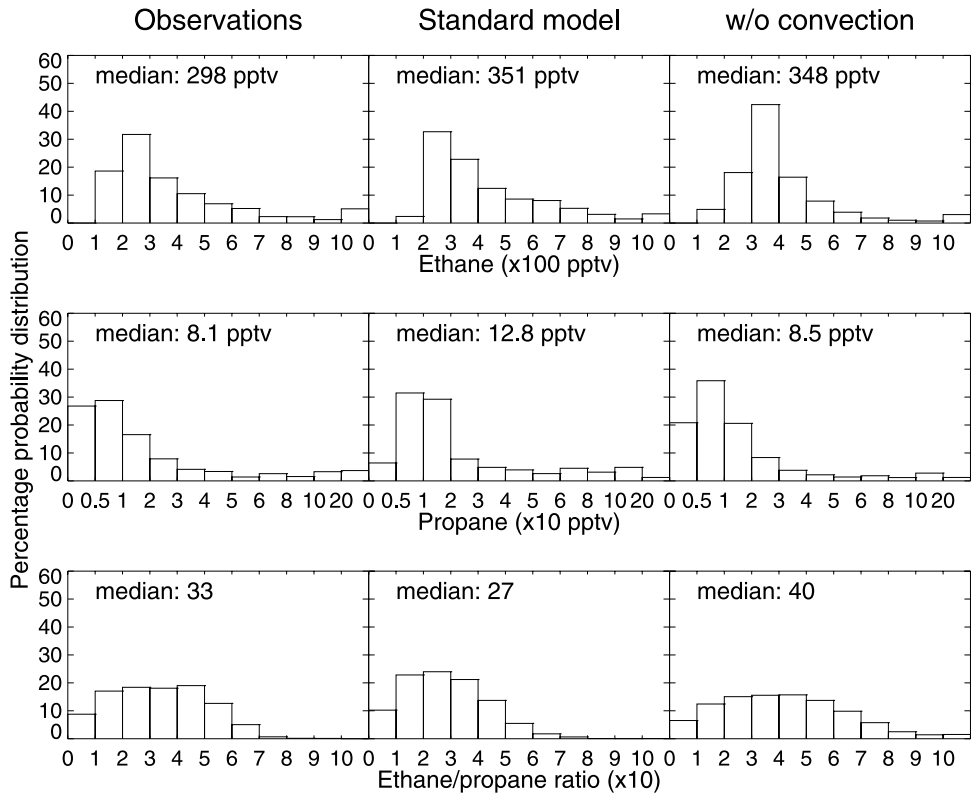

Figure 8. Observed and simulated probability distributions of ethane, propane, and ethane/propane ratio. Results from the standard model and the one without convection are shown.

as ethane and propane, the concentrations of which are not as variable as ^{222}Rn and CH_3I and the measurements of which are more reliable and widely available, can be used to evaluate the effects of convective transport in the model. The constraints placed by ethane and propane observations if any will be more sensitive to convection at northern middle latitudes, where the major sources are located.

[42] We conduct a sensitivity simulation using tagged ethane and propane tracers, in which convective transport is turned off. The model was spun for a year and the second year data were analyzed. Fifty synthetic data sets are constructed with randomly selected ethane and propane concentrations at the same locations of the observations. Mean $|\beta|$ values for the various source categories are listed in Table 1. Compared with the standard run, the $|\beta|$ values are generally lower. For the "all sources" category, there are two linear correlations as in Figure 7 but the $|\beta|$ values decrease by about 0.15 for both (not shown). The decrease can be qualitatively interpreted by suppressed mixing without convection, which leads to the decrease of $|\beta|$ toward the $|\beta|^c$ value (equation 16). Among the tagged tracer simulations for individual source regions, the large decrease (0.11–0.18) occurs for ethane and propane emitted from sources located at northern middle latitudes, including biofuel combustion and industry over North America, Europe, and northern Asia (>30°N) (Table 1). The decrease of $|\beta|$ values for these sources is consistent with the 0.15 decrease of $|\beta|$ values in the correlation of propane and ethane/propane ratio (the "all sources" category). It therefore implies that the underestimate of $|\beta|$ during PEM-Tropics B in the model (Figures 5 and 6) reflects underestimated convective transport at northern middle latitudes in the model.

5.3. Constraints of the Correlation on Latitudinal Transport From Northern Middle Latitudes to the Tropics

[43] The lifetime of ethane is about 5 times longer than propane. Therefore transport processes have different effects on the distributions of these two tracers. Figure 8 compares the probability distributions of ethane, propane, and ethane/propane ratio of the observations, the standard model, and the model without convective transport. When convective transport is disabled in the model, the propane population shifts toward lower concentrations while the ethane population shifts higher from the 200–300 pptv bin to 300–400 pptv. The opposite effects can be understood on the basis of the effective transport of ethane and propane from northern middle latitudes to the tropics through the lower-altitude branch of Hadley circulation. Propane is oxidized faster in the tropical lower troposphere, which renders convective transport critical. Disabling convective transport results in a shorter lifetime of propane in the tropics because the majority of propane stays in the lower troposphere, where its lifetime is much shorter than the middle and upper troposphere. Ethane has a much longer lifetime in comparison. Over the region of PEM-Tropics B, the accumulation of ethane at low altitudes due to the lack of convection and efficient low-altitude transport from the Northern Hemisphere to the tropical Pacific led to increasing ethane concentrations in the region. In addition, the less efficient large-scale Hadley circulation in the tropics

is still effective in transporting ethane from the lower to middle and upper troposphere where its lifetime is significantly longer. This difference is reflected in the changing distributions of ethane and propane in the tropics when convective transport is turned off (not shown). The net result is that the ethane/propane ratio is higher without convective transport.

[44] Comparing to PEM-Tropics B observations, both simulations significantly underestimate the ethane population in the 100–200 ppbv range (Figure 8), suggesting that latitudinal mixing from northern middle latitudes to the tropics is too fast. The median concentrations and the probability distributions of propane and ethane/propane ratio in the simulation without convection are closer to the observations than the standard simulations. We cannot determine if tropical convective transport is overestimated in the model because part of the error in the standard model is due to latitudinal transport.

[45] We note that it is possible that OH is underestimated in the model on the basis of Figure 8 alone. However, if we assume that transport in the model is correct, then the underestimate of $|\beta|$ value in the model (Figure 7, Table 1) implies that OH concentrations in the model would be overestimated, which contradicts the probability distribution results in Figure 8. Hence considering both the correlation between propane and ethane/propane ratio and the probability distributions is critical.

[46] While the evaluations of simulated with observed correlations of propane and ethane/propane ratio and the probability distributions provide important clues to potential defects of simulated transport processes, this approach cannot pinpoint the exact dynamic processes responsible for the defects. Additional investigations of other chemical tracers and meteorological variables are necessary. Sensitivity simulations in a coupled dynamical-chemical model would be useful to provide more insights into the effect of a particular dynamic process on the correlation and probability distribution. Using meteorological fields from multiple general circulation models in the chemical transport simulations will also provide additional information.

6. Discussion and Conclusions

[47] Our understanding of observed tracer correlations is better formulated for the stratosphere than the troposphere in part because of more complex tropospheric transport and source processes. The "slope equilibrium" developed by *Plumb and Ko* [1992] applies to long-lived species, the chemical lifetimes of which are longer than that of quasi-horizontal transport, in the stratosphere. The correlation under such conditions reflects the parallelization of constant mixing ratio surfaces of the two tracers in the altitude-latitude space. A key characteristic of these correlations is that they exist in the linear space of mixing ratios.

[48] Observational evidence shows that tropospheric chemical tracers are often strongly correlated. In contrast to the stratospheric tracer correlations in the linear space, the tropospheric tracer correlations usually exist in the log space of mixing ratios [e.g., *Parrish et al.*, 1992; *McKeen et al.*, 1996]. The resulting slopes are often close to the ratio of reaction rate constants of their major oxidation pathways. The assumptions that can be made for long-lived stratospheric tracers are invalid in the troposphere. In this study, we attempt to provide an alternative framework to understand tropospheric tracer correlations.

[49] We choose to examine the correlation between ethane and propane in part because their sources (mainly industry-related) are reasonably well defined and in part because they are oxidized mainly by OH and have negligible reactions with NO_3 or halogen radicals. The OH oxidation has a temperature dependence that can complicate the interpretation of the correlation. To minimize the temperature effect, we choose to examine the correlation between propane and ethane/propane ratio. Furthermore, propane and ethane/propane ratio respond differently when mixing with clean background air is considered [*Parrish et al.*, 1992] and hence their correlation is more sensitive to mixing than that between ethane and propane. The absolute value of kinetics correlation slope, $|\beta|^c$ (equation (4)), is 1.24 ± 0.07 under tropospheric conditions.

[50] Previous studies [e.g., *McKeen and Liu*, 1993] have shown that the correlation is a function of OH oxidation and mixing. The approach by *McKeen et al.* [1996] has two difficulties: (1) a constant background concentration for mixing with plumes is often difficult to define, and (2) the formulation does not land itself to a linear correlation in the log space of mixing ratios, especially when the background concentrations are relatively high.

[51] We propose an alternative "finite-mixing" model, in which high turbulent mixing regions are bounded by low turbulent mixing regions. With our assumption, the mixing ratio decay of a tracer in the plume with time is defined by $\exp(-\lambda l_c t)$, where l_c is the first-order chemical loss rate constant and λ is an augmentation factor due to mixing. While the complexity of tropospheric processes precludes more rigorous analysis as done by *Plumb and Ko* [1992] for the stratosphere, the empirical formulation helps the physical interpretation of the observations and model results. A direct consequence of the formulation is that the correlation slope $|\beta|$ of propane and ethane/propane ratio in log space is the sum of the kinetics slope value $|\beta|^c$ and the differential mixing augmentation between the two tracers, $\frac{(\lambda_1/\lambda_2 - 1)k_1}{k_2 - k_1}|\beta|^c$ (equation (16)), where k_1 and k_2 are the second-order reaction rate constants for OH oxidation of ethane and propane, respectively. For tracer pairs like ethane and propane, where k_2 is much larger than k_1, the deviation from the kinetics slope tends to be small. As a result, the linear correlation often looks as if it were purely driven by differential photochemical loss, which may explain why the mixing processes are often ignored [e.g., *McKeen et al.*, 1990].

[52] To test what additional insight can be learnt from investigating the correlation between propane and ethane/propane ratio, we examine the observations and GEOS-CHEM simulations for the northern middle and high latitudes (TOPSE) and tropical Pacific (PEM-Tropics B). Photochemically aged air masses were sampled in these missions.

[53] TOPSE observations at northern middle and high latitudes in spring show a clear decrease of $|\beta|$ values from February/March to May, reflecting in part the increasing photochemical activity in spring. The lower values of $|\beta|$ at high latitudes than middle latitudes suggest a stronger dynamic isolation at high latitudes since photochemistry is

much more active at middle latitudes. GEOS-CHEM simulations show a large decrease in April but an increase in May. In the meantime, the probability distribution of ethane/propane ratio shows a large overestimate in May at middle latitudes. If OH were overestimated in the model leading to the overestimate of ethane/propane ratio, we would expect a lower $|\beta|$ value. Therefore the overestimate of $|\beta|$ values at middle latitudes in May reflects an overestimate of mixing possibly due to excessive transport from lower latitudes in the model. We hypothesize that the overestimate of $|\beta|$ at high latitudes reflects excessive horizontal mixing possibly as a result of model underestimate of convection.

[54] Over the tropical Pacific, both the observations and the model show the two-branch structure in the linear correlations of propane and ethane/propane ratio in log space. Data points for the minor branch were observed mostly in the southern subtropics and middle latitudes. This feature is well reproduced in the model. The minor branch results from different transport and chemistry coupling characteristics in the Southern from Northern Hemispheres.

[55] To evaluate the effect of source location, tagged tracers are simulated for emissions from biomass burning, biofuel combustions, and industrial sources in North America, Europe, northern Asia (north of 30°N), southern Asia (south of 30°N), South America, northern Africa (north of the equator), southern Africa (south of the equator) and Australia. The $|\beta|$ values are clearly lower for emissions from the southern tropics, reflecting higher OH concentrations in the tropics. Considering the regional nature of the coupling between chemistry and transport and the vastly different strengths of various sources, the existence of only two relatively well-defined linear correlations reflects the effective homogenization by tropospheric mixing processes.

[56] The simulated $|\beta|$ value for the major correlation line is lower than observed suggesting that mixing is overestimated relative to photochemical oxidation. One transport process that can be easily modified in the model is convection. When convection is turned off, the simulated $|\beta|$ values decrease as expected. The underestimate of $|\beta|$ values in the model therefore appears to imply that convective transport is underestimated in the model at northern middle latitudes, where the major ethane and propane sources are located. Our approach therefore can be used as an alternative method to directly evaluate model convective transport in addition to using short-lived chemical tracers such as ^{222}Rn and CH_3I. The comparison of observed and simulated probability distributions of ethane, propane, and ethane/propane ratio indicate that the simulated ethane and propane concentrations tend to be higher and simulated ethane/propane ratios tend to be lower, implying that transport from northern middle latitudes into the tropical Pacific is overestimated in the model.

[57] We show that the correlation of propane and ethane/propane ratio and the probability distributions can be used as a metric for defining the subset of observations that are appropriate for inverse modeling. The underestimate of the $|\beta|$ value over tropical Pacific during PEM-Tropics B suggests that the discrepancy between model and observations is due to systematic (not random) model transport biases. As a result, the inverse modeling results will also be systematically biased. For TOPSE observations, we find that the simulated and observed $|\beta|$ values are in good agreement in March at middle latitudes and in February–April at high latitudes. The observed and simulated probability distributions of ethane/propane ratio are also in agreement for these data. We find that ethane and propane emissions in the model are underestimated by 14 ± 5% on the basis of these data.

[58] **Acknowledgments.** We thank Donald Blake's group for their measurements of ethane and propane. The GEOS-CHEM model is managed at Harvard University with support from the NASA Atmospheric Chemistry Modeling and Analysis Program. We thank Robert Yantosca and Daniel Jacob for providing us the model and data. This work was supported by the NASA ACMAP program and NSF atmospheric chemistry program.

References

Arellano, A. F., Jr., P. S. Kasibhatla, L. Giglio, G. R. van der Werf, and J. T. Randerson (2004), Top-down estimates of global CO sources using MOPITT measurements, *Geophys. Res. Lett.*, *31*, L01104, doi:10.1029/2003GL018609.

Atlas, E. L., B. A. Ridley, and C. A. Cantrell (2003), The Tropospheric Ozone Production about the Spring Equinox (TOPSE) Experiment: Introduction, *J. Geophys. Res.*, *108*(D4), 8353, doi:10.1029/2002JD003172.

Avallone, L. M., and M. J. Prather (1997), Tracer-tracer correlations: Three-dimensional model simulations and comparisons to observations, *J. Geophys. Res.*, *102*, 19,233–19,246.

Bell, N., L. Hsu, D. J. Jacob, M. G. Schultz, D. R. Blake, J. H. Butler, D. B. King, J. M. Lobert, and E. Maier-Reimer (2002), Methyl iodide: Atmospheric budget and use as a tracer of marine convection in global models, *J. Geophys. Res.*, *107*(D17), 4340, doi:10.1029/2001JD001151.

Bey, I., D. J. Jacob, R. M. Yantosca, J. A. Logan, B. Field, A. M. Fiore, Q. Li, H. Liu, L. J. Mickley, and M. Schultz (2001), Global modeling of tropospheric chemistry with assimilated meteorology: Model description and evaluation, *J. Geophys. Res.*, *106*, 23,073–23,096.

Blake, N. J., et al. (2001), Large-scale latitudinal and vertical distributions of NMHCs and selected halocarbons in the troposphere over the Pacific Ocean during the March–April 1999 Pacific Exploratory Mission (PEM-Tropics B), *J. Geophys. Res.*, *106*, 32,627–32,644.

Blake, N. J., D. R. Blake, B. C. Sive, A. S. Katzenstein, S. Meinardi, O. W. Wingenter, E. L. Atlas, F. Flocke, B. A. Ridley, and F. S. Rowland (2003), NMHCs and halocarbons in Asian Continental Outflow during TRACE-P: Comparison to PEM-West B, *J. Geophys. Res.*, *108*(D20), 8806, doi:10.1029/2002JD003367.

Browell, E. V., et al. (2003), Ozone, aerosol, potential vorticity, and trace gas trends observed at high latitudes over North America from February to May 2000, *J. Geophys. Res.*, *108*(D4), 8369, doi:10.1029/2001JD001390.

Cantrell, C. A., et al. (2003), Steady state free radical budgets and ozone photochemistry during TOPSE, *J. Geophys. Res.*, *108*(D4), 8361, doi:10.1029/2002JD002198.

Duncan, B. N., R. V. Martin, A. C. Staudt, R. Yevich, and J. A. Logan (2003), Interannual and seasonal variability of biomass burning emissions constrained by satellite observations, *J. Geophys. Res.*, *108*(D2), 4100, doi:10.1029/2002JD002378.

Ehhalt, D. H., F. Rohrer, A. Wahner, M. J. Prather, and D. R. Blake (1998), On the use of hydrocarbons for the determination of tropospheric OH concentrations, *J. Geophys. Res.*, *103*, 18,981–18,997.

Evans, M. J., et al. (2003), Coupled evolution of BrO_x-ClO_x-HO_x-NO_x chemistry during bromine-catalyzed ozone depletion events in the arctic boundary layer, *J. Geophys. Res.*, *108*(D4), 8368, doi:10.1029/2002JD002732.

Goldstein, A. H., S. C. Wofsy, and C. M. Spivakovsky (1995), Seasonal variations of nonmethane hydrocarbons in rural New England: Constraints on OH concentrations in northern midlatitudes, *J. Geophys. Res.*, *100*, 21,023–21,033.

Hoell, J. M., D. D. Davis, D. J. Jacob, M. O. Rodgers, R. E. Newell, H. E. Fuelberg, R. J. McNeal, J. L. Raper, and R. J. Bendura (1999), The Pacific Exploratory Mission in the tropical Pacific: PEM-Tropics A, August–September 1996, *J. Geophys. Res.*, *104*, 5567–5583.

Jacob, D. J., et al. (1997), Evaluation and intercomparison of global atmospheric transport models using radon-222 and other short-lived tracers, *J. Geophys. Res.*, *102*, 5953–5970.

Jacob, D. J., J. Crawford, M. M. Kleb, V. S. Connors, R. J. Bendura, J. L. Raper, G. W. Sachse, J. Gille, L. Emmons, and J. C. Heald (2003), Transport and chemical evolution over the Pacific (TRACE-P) mission: Design, execution, and first results, *J. Geophys. Res.*, *108*(D20), 9000, doi:10.1029/2002JD003276.

Jobson, B. T., et al. (1998), Spatial and temporal variability of nonmethane hydrocarbon mixing ratios and their relation to photochemical lifetime, *J. Geophys. Res.*, *103*, 13,557–13,567.

Jobson, B. T., et al. (1999), Trace gas mixing ratio variability versus lifetime in the troposphere and stratosphere: Observations, *J. Geophys. Res.*, *104*, 16,091–16,113.

Junge, C. E. (1974), Residence time and variability of tropospheric trace gases, *Tellus*, *26*, 477–488.

McKeen, S. A., and S. C. Liu (1993), Hydrocarbon ratios and photochemical history of air masses, *Geophys. Res. Lett.*, *20*, 2363–2366.

McKeen, S. A., M. Trainer, E. Y. Hsie, R. K. Tallamraju, and S. C. Liu (1990), On the indirect determination of atmospheric OH radical concentrations from reactive hydrocarbon measurements, *J. Geophys. Res.*, *95*, 7493–7500.

McKeen, S. A., S. C. Liu, E.-Y. Hsie, X. Lin, J. D. Bradshaw, S. Smyth, G. L. Gregory, and D. R. Blake (1996), Hydrocarbon ratios during PEM-West A: A model perspective, *J. Geophys. Res.*, *101*, 2087–2109.

McKenna, D. S. (1997), Analytic solutions of reaction diffusion equations and implications for the concept of an air parcel, *J. Geophys. Res.*, *102*, 13,719–13,725.

Palmer, P. I., D. J. Jacob, A. M. Fiore, R. V. Martin, K. Chance, and T. P. Kurosu (2003), Mapping isoprene emissions over North America using formaldehyde column observations from space, *J. Geophys. Res.*, *108*(D6), 4180, doi:10.1029/2002JD002153.

Parrish, D. D., C. J. Hahn, E. J. Williams, R. B. Norton, and F. C. Fehsenfeld (1992), Indications of photochemical histories of Pacific air masses from measurements of atmospheric trace species at Point Arena, California, *J. Geophys. Res.*, *97*, 15,883–15,901.

Penkett, S. A., N. J. Blake, P. Lightman, A. R. W. Marsh, P. Anwyl, and G. Butcher (1993), The seasonal variation of nonmethane hydrocarbons in the free troposphere over the North Atlantic Ocean: Possible evidence for extensive reaction of hydrocarbons with the nitrate radical, *J. Geophys. Res.*, *98*, 2865–2885.

Plumb, R. A., and M. K. W. Ko (1992), Interrelationships between mixing ratios of long-lived stratospheric constitutes, *J. Geophys. Res.*, *97*, 10,145–10,156.

Raper, J. L., M. M. Kleb, D. J. Jacob, D. D. Davis, R. E. Newell, H. E. Fuelberg, R. J. Bendura, J. M. Hoell, and R. J. McNeal (2001), Pacific Exploratory Mission in the tropical Pacific: PEM-Tropics B, March–April 1999, *J. Geophys. Res.*, *106*, 32,401–32,425.

Ridley, B. A., et al. (2003), Ozone depletion events observed in the high latitude surface layer during the TOPSE aircraft program, *J. Geophys. Res.*, *108*(D4), 8356, doi:10.1029/2001JD001507.

Sander, S. P., A. R. Ravishankara, D. M. Golden, C. E. Kolb, M. J. Kurylo, M. J. Molina, G. K. Moortgat, and B. J. Finlayson-Pitts (2003), Chemical kinetics and photochemical data for use in stratospheric modeling, *JPL Publ. 02-25, Eval., 14*, Jet Propulsion Lab., Pasadena, Calif.

Schultz, M., et al. (1999), On the origin of tropospheric ozone and NOx over the tropical South Pacific, *J. Geophys. Res.*, *104*, 5829–5843.

Seinfeld, J. H., and S. N. Pandis (1998), *Atmospheric Chemistry and physics: From Air Pollution to Climate Change*, 1326 pp., John Wiley, Hoboken, N. J.

Talbot, R. W., J. E. Dibb, E. M. Scheuer, D. R. Blake, N. J. Blake, G. L. Gregory, G. W. Sachse, J. B. Bradshaw, S. T. Sandholm, and H. B. Singh (1999), Influence of biomass combustion emissions on the distribution of acidic trace gases over the southern Pacific basin during austral springtime, *J. Geophys. Res.*, *104*, 5623–5634.

Wang, Y., D. J. Jacob, and J. A. Logan (1998a), Global simulation of tropospheric O_3-NO_x-hydrocarbon chemistry: 1. Model formulation, *J. Geophys. Res.*, *103*, 10,713–10,725.

Wang, Y., J. A. Logan, and D. J. Jacob (1998b), Global simulation of tropospheric O_3-NO_x-hydrocarbon chemistry: 2. Model evaluation and global ozone budget, *J. Geophys. Res.*, *103*, 10,727–10,755.

Wang, Y., S. C. Liu, H. Yu, S. Sandholm, T.-Y. Chen, and D. R. Blake (2000), Influence of convection and biomass burning on tropospheric chemistry over the tropical Pacific, *J. Geophys. Res.*, *105*, 9321–9333.

Wang, Y., et al. (2001), Factors controlling tropospheric O_3, OH, NO_x, and SO_2 over the tropical Pacific during PEM-Tropics B, *J. Geophys. Res.*, *106*, 32,733–32,748.

Wang, Y., et al. (2003a), Springtime photochemistry at northern middle and high latitudes, *J. Geophys. Res.*, *108*(D4), 8358, doi:10.1029/2002JD002227.

Wang, Y., et al. (2003b), Intercontinental transport of pollution manifested in the variability and seasonal trend of springtime O_3 at northern middle and high latitudes, *J. Geophys. Res.*, *108*(D21), 4683, doi:10.1029/2003JD003592.

Xiao, Y., D. J. Jacob, J. S. Wang, J. A. Logan, P. I. Palmer, P. Suntharalingam, R. M. Yantosca, G. W. Sachse, D. R. Blake, and D. G. Streets (2004), Constraints on Asian and European sources of methane from CH_4-C_2H_6-CO correlations in Asian outflow, *J. Geophys. Res.*, *109*, D15S16, doi:10.1029/2003JD004475.

Yevich, R., and J. A. Logan (2003), An assessment of biofuel use and burning of agricultural waste in the developing world, *Global Biogeochem. Cycles*, *17*(4), 1095, doi:10.1029/2002GB001952.

Zeng, T., Y. Wang, K. Chance, E. V. Browell, B. A. Ridley, and E. L. Atlas (2003), Widespread persistent near-surface ozone depletion at northern high latitudes in spring, *Geophys. Res. Lett.*, *30*(24), 2298, doi:10.1029/2003GL018587.

Y. Wang and T. Zeng, School of Earth and Atmospheric Sciences, Georgia Institute of Technology, Atlanta, GA 30332-0340, USA. (ywang@eas.gatech.edu)